

Optical resonances of indium islands on GaAs(001) observed by reflectance anisotropy spectroscopy

N. Esser,^{1,*} A. M. Frisch,¹ A. Röseler,² S. Schintke,³ C. Goletti,⁴ and B. O. Fimland⁵

¹*Institut für Festkörperphysik, Technische Universität Berlin, Hardenbergstraße 36, D-10623 Berlin, Germany*

²*Institut für Spektrochemie und Angewandte Spektroskopie, Institutsteil Berlin-Adlershof, D-12498 Berlin, Germany*

³*NCCR on Nanoscale Science, Institut für Physik, Universität Basel, Klingelbergstrasse 82, CH-4056 Basel, Switzerland*

⁴*Physics Department and INFN, Università di Roma "Tor Vergata," Via della Ricerca Scientifica 1, 00133 Roma, Italy*

⁵*Department of Physical Electronics, Norwegian University of Science and Technology, NO-7491 Trondheim, Norway*

(Received 22 October 2002; published 17 March 2003)

The optical properties of indium islands on GaAs(001) surfaces have been studied by reflectance anisotropy spectroscopy as a function of metal coverage. A large optical anisotropy is observed, which shows an oscillatory behavior and scales with the island size: mean island sizes determined by scanning electron microscope correspond to the wavelengths where extremes in the optical anisotropy arise. We explain this behavior by surface plasmon resonances of the island structure which induce a huge optical anisotropy related to the anisotropic shape and distribution of the In islands. Model calculations of the reflectance anisotropy spectroscopy signal based on a layer system where the island film is represented by an effective medium consisting of ellipsoidal metal particles in a vacuum matrix reproduce the main oscillation and support our conclusion.

DOI: 10.1103/PhysRevB.67.125306

PACS number(s): 78.20.Ci, 78.66.Bz

I. INTRODUCTION

Mie resonances, or so-called morphology dependent resonances of electromagnetic waves in metallic and dielectric particles have been subject to intense investigations with optical spectroscopy for a long time.¹⁻³ Such resonances are, for example, readily observed in extinction/absorption cross sections or the angular distribution of scattered light. Resonance frequencies for transverse electric and transverse magnetic modes depend on shape, size, and material properties (i.e., refractive index or dielectric function) of the particles. For particle sizes much smaller than the wavelength, only the first-order multipole, i.e., the dipole is resonantly excited. Scattering can therefore be described in the so-called Rayleigh limit. With increasing particle size or with an increasing size parameter ka approaching 1, higher-order multipoles become resonantly excited leading to the so-called Mie regime of reflected and scattered light waves. Here, a represents the particle size, λ is the wavelength of the exciting electromagnetic radiation, and k is the wave vector defined as $k = 2\pi/\lambda$. In the past few years, the use of these resonances for resonance enhanced spectroscopy, due to the high local-field enhancement at the surfaces of the particles, and the potential of Mie resonances for optical size analysis have attracted considerable interest.⁴

In this paper, we report on optical resonances in the Mie regime ($ka \approx 1$) detected by the polarization state of light, a topic hardly studied so far. The polarization state of the light backscattered from metal islands on a semiconductor surface has been determined by reflectance anisotropy spectroscopy (RAS). This method measures, similar to spectroscopic ellipsometry, the difference in the complex reflectivity for two light waves of same intensity but with perpendicular polarization directions, but under near-normal incidence. RAS has been established in recent years for the optical study of semiconductor surfaces and *in situ* optical monitoring of semi-

conductor growth.⁵⁻⁷ More recently, the potential of RAS for studying other materials, for example, metal surfaces, has been exploited as well.⁸⁻¹¹

As will be shown, metallic islands such as In can give rise to a huge optical anisotropy due to an anisotropic island morphology. For In on GaAs(001), the morphology related optical anisotropy is two orders of magnitude larger than that related to the surface structure of the GaAs substrate. The inequivalent crystal directions within the In-island covered (001) surface correspond to the $[1\bar{1}0]$ and $[110]$ directions, just as in the case of a clean GaAs(001) surface. We ascribe the optical anisotropy to a small average anisotropy of the island shapes and the strong enhancement to surface-plasmon resonances induced by rather uniform sizes of the In islands. Thus, using RAS, a simple quantitatively reliable optical spectroscopy technique that does not require any reference spectra is available for the determination of the size parameters controlling the island morphology.

II. EXPERIMENT

A. Sample preparation

Samples were prepared by indium deposition on clean reconstructed (001) surfaces of GaAs substrates in ultrahigh vacuum (UHV) (base pressure: 4×10^{-11} mbar). First, a slightly doped ($n_{Si} = 10^{16} \text{ cm}^{-3}$) GaAs buffer layer was grown on GaAs(001) substrates by molecular-beam epitaxy. This buffer layer was capped by an amorphous arsenic cap layer after growth. After transfer of the samples through ambient conditions into UHV, the cap layer was removed from the surfaces by heating to ≈ 450 °C (decapping). The resulting clean surfaces were *in situ* analyzed by low-energy electron diffraction (LEED), Auger electron spectroscopy (AES), scanning tunneling microscopy, and RAS.¹²⁻¹⁴ After decapping, the surfaces showed a (2×4) LEED pattern that is associated with the well-known arsenic-rich reconstruction of

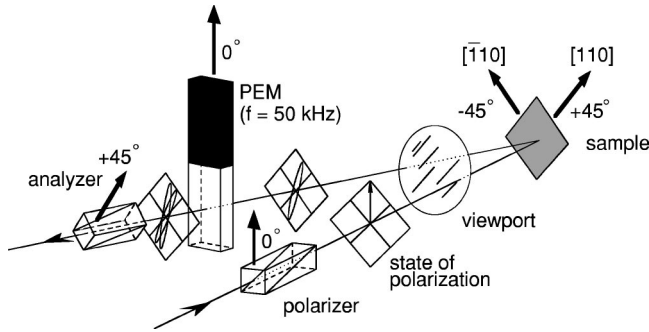


FIG. 1. RAS setup used for polarization analysis of reflected light under near-normal incidence. Rochon prisms (polarizer and analyzer) and the photoelastic modulator are commercial elements made of UV-grade quartz (Ref. 17).

the surface.¹³ No contaminations with carbon or oxygen could be determined by AES. Indium was deposited directly onto the clean, reconstructed surfaces in UHV. The deposition was carried out at room temperature by thermal evaporation of indium from a Knudsen cell at a deposition rate of 0.1 ML/s (ML stands for monolayer). The deposition rate was controlled by a calibrated quartz microbalance. The background pressure during deposition remained below 1×10^{-10} mbar. The optical anisotropy of the surfaces was then examined in UHV (*in situ*) as well as after removal from UHV to ambient conditions (*ex situ*) by reflectance anisotropy spectroscopy. Indium deposition in the submonolayer regime is known to modify the GaAs(001) surface structure in a defined manner and to give rise to characteristic changes in the optical anisotropy.^{12,14} While the anisotropy related to the surface structure (clean or indium terminated) is immediately quenched upon contact with air, the In-island related resonances described here remain unaffected.

Island sizes, shapes, and distributions were determined *ex situ* by scanning electron microscopy (SEM). These results have been reported in Refs. 15 and 16.

B. Reflectance anisotropy spectroscopy

The experimental setup for reflectance anisotropy spectroscopy is shown in Fig. 1. A detailed description can be found in Refs. 6 and 17. Two different RAS setups were used, one with an incidence angle of around 2.5° and one with an incidence angle below 1° . Typically, the diameter of the illuminated area on the sample is around 0.5–1 cm. Thus, in our experiments, the sampling area corresponds to the whole surface of the GaAs sample. The reflectance anisotropy is defined as¹⁷

$$\frac{\Delta r}{r} = \frac{r_1 - r_2}{\langle r \rangle}, \quad (1)$$

where r_1 and r_2 stand for the complex amplitude reflection coefficient of linear polarized light along two perpendicular directions denoted 1 and 2, and $\langle r \rangle$ is the average of both quantities. In case of the surface of a solid, for example, the (001) surface of GaAs, directions 1 and 2 are chosen such

that they correspond to crystallographic directions along the crystal surface which are inequivalent as regards to their symmetry properties. For the (001) surface of GaAs, these are the $[110]$ and $[\bar{1}10]$ directions. Since GaAs has a cubic bulk crystal structure (zinc blende structure), the difference between r_1 and r_2 is solely related to the surface layer, irrespective of the much larger light penetration depth. Note that it is only in the case of optically isotropic materials, for example, GaAs, that the optical anisotropy is exclusively related to the surface. In the case of crystals with lower symmetry, the majority of the optical anisotropy may arise from the bulk. Another possible source of optical anisotropy is the morphology of surfaces, a topic not much studied so far. In many cases, epitaxial growth gives rise to islands of anisotropic shape. In this case, as we will show, the island morphology rather than the optical properties of the island material gives rise to an optical anisotropy.

III. EXPERIMENTAL RESULTS

A. Island sizes, shapes, and distribution

The epitaxial growth of indium on GaAs(001) surfaces has previously been investigated by AES, SEM, and x-ray reflection diffraction (XRD).^{15,16} Here, only the main results will be briefly reviewed: The shape of indium islands growing on the (2×4) GaAs(001) surface changes with coverage. Up to 130 ML, islands have a regular shape with a rectangular base. The island edges are oriented along the $[110]$ and $[\bar{1}10]$ directions of the GaAs(001) surface. A slow attenuation of Ga and As Auger lines indicates an increasing size of three-dimensional (3D) islands with coverage rather than 2D substrate covering. Above 130 ML of In, the growth mode changes, as indicated by an even weaker Auger attenuation. In this coverage regime, large In islands surrounded by smaller ones are found in SEM images. Most likely, the large islands have been generated by coalescence of the former small ones, the latter being still present in intermediate regions where no coalescence has occurred yet. The shape of the large islands can be described by an obelisk with a rectangular shaped base, whose edges are still oriented along the $[110]$ and $[\bar{1}10]$ directions of the GaAs(001) surface. The indium islands show a uniform size distribution with their mean size increasing with coverage. As an example, SEM images for 270 ML and 1000 ML of In on GaAs(001) are shown in Fig. 2. For coverages above 700 ML, the large islands coalesce, leading to rather irregular island shapes and quite different island sizes for a given In coverage. The crystalline structure of the indium islands is face-centered tetragonal. XRD measurements of 2000 ML of indium show that the (001), (010), and (111) planes are oriented parallel to the surface at ratios of $\approx 6:1:1$, indicating a preferential island growth in the epitaxial (001) orientation. Therefore, the side faces of the obelisk like In islands are most likely (111) crystal planes.

B. Reflectance anisotropy spectroscopy

As mentioned in Sec. I, clean and indium submonolayer terminated GaAs(001) surfaces have been investigated

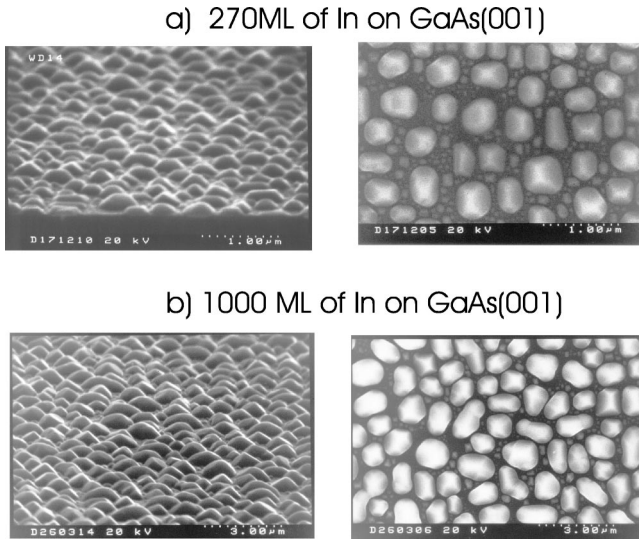


FIG. 2. SEM micrographs of indium islands (top view and 75° side view) on the (001) surface of GaAs for two different In coverages: (a) 270 ML (upper panel) and (b) 1000 ML (lower panel). Please note the different length scales indicated in the SEM micrographs.

previously.^{7,14} RAS spectra and their correlation to the atomic surface structure, or reconstruction, are thus well known. However, above a minimum In coverage of ≈ 100 ML, the formation of indium islands on the GaAs(001) surface leads to RAS spectra which are totally different in shape and amplitude as compared to the surface related optical anisotropy, and whose correlation to the surface morphology is presently not well understood. Figure 3 shows two RAS

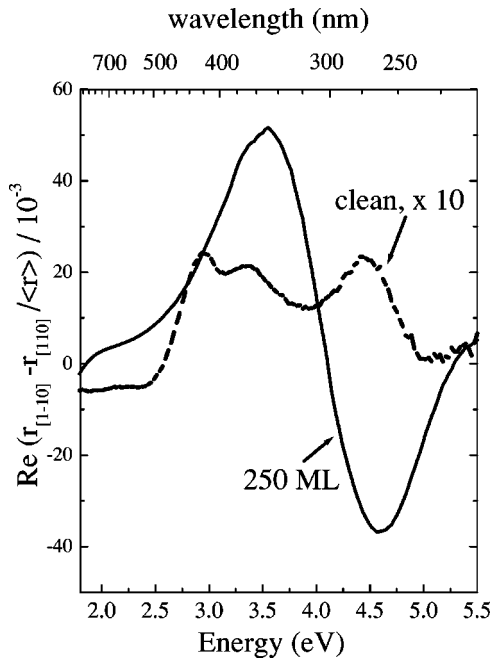


FIG. 3. RAS spectra of a clean GaAs(001) surface of (2×4) reconstruction (dashed line) and the same sample after deposition of 250 ML of In (full line). The spectrum of the clean surface has been scaled by a factor of 10.

spectra, the typical one related to a clean GaAs(001) surface with (2×4) reconstruction, and one obtained after deposition of 250 ML of In. The giant amplitude of the spectrum related to the In-covered sample as compared to that of the clean sample is evident at first sight. [Please note that the spectrum of clean GaAs(001) is enhanced by a factor of 10.] Also the shape of the anisotropy spectrum of the In covered sample is very unusual: a rather symmetric minimum-maximum structure centered around 4 eV can be seen. Particularly remarkable is the dependence of the RAS spectra on In coverage. Figure 4 shows the real parts of RAS spectra from GaAs(001) surfaces with increasing coverage (100–1000 ML) of indium. In Fig. 4(a), the spectra are shown as a function of photon energy, as usual, whereas Fig. 4(b) shows the same spectra as a function of wavelength. For a nominal coverage of 100 ML of indium, a large and broad positive optical anisotropy at the high-energy (short wavelength) cutoff of the RAS spectrum shows up. With increasing coverage, the position of the maximum optical anisotropy shifts to lower energy (longer wavelengths) and for a coverage of 150 ML, an additional minimum appears at the high-energy (short wavelength) cutoff. Minimum and maximum positions shift with the coverage to lower energies (longer wavelengths) leading to an oscillator-like form of the RAS line shape. For higher coverage, another maximum and finally another minimum moves from the high-energy (short wavelength) cutoff into the accessible spectral range of the RAS apparatus. In Fig. 4(b), the maxima and minima are labeled by “1,” “2,” “3,” and “4” according to their appearance with increasing In coverage. Since the RAS signal is given by the difference of the reflection for light polarization along $[1\bar{1}0]$ and $[110]$ (normalized to the average reflectivity), a positive RAS signal corresponds to $r[1\bar{1}0] > r[110]$ and a negative one to $r[1\bar{1}0] < r[110]$.

The spectral positions of the extrema 1, 2, and 3 as a function of In coverage are shown in Fig. 5. An approximately linear dependence of the wavelength positions on the coverage in the ML is observed for the first maximum 1 ($r[1\bar{1}0] > r[110]$), the first minimum 2 ($r[1\bar{1}0] < r[110]$), and the second maximum 3 ($r[1\bar{1}0] > r[110]$) up to 600 ML of In coverage. The wavelength position of the leading maximum 1 is approximately equal to the mean island size determined by SEM. The spectral position of maximum 3 corresponds to half of the wavelength of maximum 1. The line shape of the RAS spectra changes, with increasing coverage from an oscillation with nearly equal amplitudes of maxima and minima shown in the two upper plots of Fig. 4(a), to oscillations with different amplitudes shown in the lower two plots of Fig. 4(a). This is due to the fact that the amplitude of the oscillations is larger in the ultraviolet range than in the visible spectral range. The amplitudes of the oscillations are highest for wavelengths between 250 nm and 500 nm and decrease for wavelengths above 500 nm. For a coverage above 800 ML, the oscillations are broadened and damped and the whole spectrum shifts to negative anisotropy.

IV. DISCUSSION OF OPTICAL ANISOTROPY

As already mentioned in the Introduction, RAS measures the difference in reflection for two light waves of right-

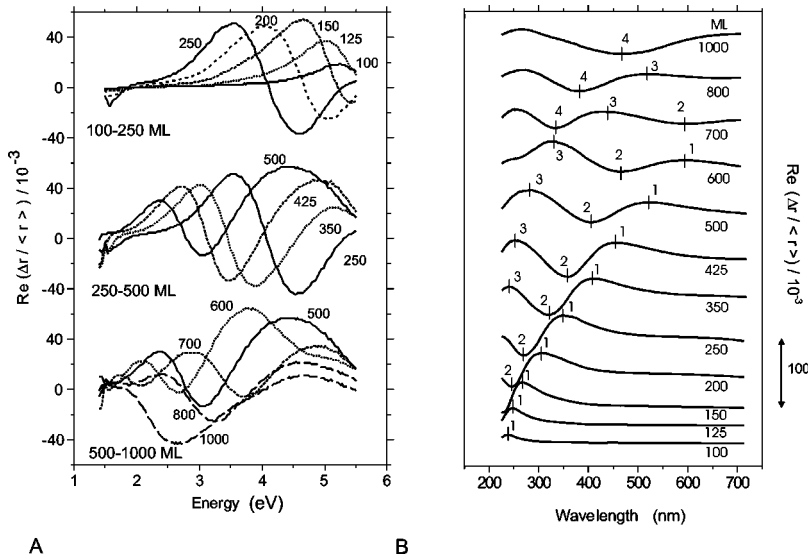


FIG. 4. RAS spectra of indium islands on the (001) surface of GaAs for different indium coverages. (a) RAS spectra as a function of photon energy; (b) RAS spectra as a function of wavelength.

angled polarization directions under nearly normal incidence. Since there is a small but finite deviation of a few degrees in the incidence angle from normal incidence, one might suspect that a difference in geometrical resonance conditions for *s*- and *p*-polarized light is responsible for the observation.⁴ This assumption was checked by measuring the dependence of the RAS spectra of one sample for (i) different incidence and reflection angles of the light and ii) for different angles between the right-angled polarization vectors of the light and the surface directions [110] and $\bar{1}\bar{1}0$. The results can be summed up as follows: (a) neither the amplitudes nor the positions of the maxima and respective minima depend on the incidence angle and (b) by rotating the sample 45° around the normal to the sample surface, the optical anisotropy vanishes completely and by rotating 90° it reverses sign. The difference between *s* and *p* polarizations therefore cannot be the source of the optical anisotropy observed. It is

evident that the optical anisotropy observed for the In-island covered GaAs is related to an anisotropy occurring between the $\bar{1}\bar{1}0$ and [110] directions.

There may be two fundamentally distinct origins of such an anisotropy: a geometric response due to an anisotropic island shape, size, or distance, or alternatively, an anisotropic dielectric response of the island material due to its crystalline structure might give rise to an optical anisotropy. A small dielectric anisotropy is expected for indium crystals due to the tetragonal crystal structure. However, this anisotropy cannot account for the observed behavior, since in the epitaxial (001) orientation as revealed by XRD, the dielectric anisotropy does not show up. Moreover, the fact that the maxima and minima shift across the entire spectral range, from 1.5 eV to 5.5 eV, dependent of the deposited amount or island size, proves that the observed oscillations cannot be related to material properties of crystalline indium. Therefore, the anisotropy of the bulk dielectric function of crystalline indium certainly does not explain our observation.

On the other hand, an anisotropic island shape (i.e., a rectangular base area) is in fact observed by SEM. However, the available SEM images show that the islands are oriented with their longer island side partially along the $\bar{1}\bar{1}0$ direction and partially along the [110] direction. Therefore, the optical anisotropy corresponds to a mean anisotropy arising by averaging over the many In islands present within the large illuminated area. Moreover, the shape of the islands and the distance in between may influence the optical anisotropy as well. For instance, the angle between the island side faces and the GaAs surface may differ for the $\bar{1}\bar{1}0$ and [110] directions. A detailed understanding of the optical anisotropy would be quite a formidable task. However, we want to point out that the RAS oscillations are observed under similar preparation conditions on a variety of different samples with very high reproducibility. Therefore, any artifact is safely excluded. We thus conclude that either the mean size, the shape of the islands, or the distance in between is anisotropic, i.e., differs slightly along the $\bar{1}\bar{1}0$ and [110] directions for the GaAs(001) substrate. A possible mi-

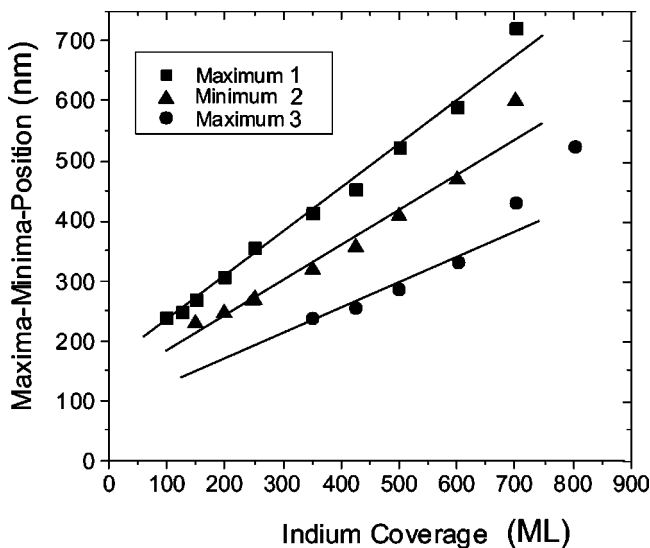


FIG. 5. Wavelength positions of maxima and minima in the RAS spectra as a function of nominal indium coverage. Straight lines are a guide to the eye.

crossopic mechanism is the anisotropic diffusion velocity of indium along the two different directions in the surface.¹² Such an anisotropic diffusion is known to exist on GaAs(001)(2×4) and was quantitatively determined for Ga adsorption.¹⁸

With this explanation for the source of optical anisotropy, the huge magnitude and the line shape of the RAS oscillations can be explained by the surface-plasmon resonances, or as Mie resonances within the generalized Mie theory.^{20,21} Due to the anisotropy in island size, shape, or distance, the resonance wavelength (or photon energy) differ slightly for $[\bar{1}\bar{1}0]$ - and $[110]$ polarized light, thus producing a 1-2-maximum-minimum structure in the RAS spectrum. The following structures correspond to higher order (multipole) Mie resonances. The position of maxima and respective minima in the spectra should then depend linearly to the first order, on the island size, which is indeed observed (see Fig. 5). The dependence of the oscillation amplitude on wavelength, i.e., finding that the oscillation amplitude in the visible range is lower than in the UV spectral range [see Fig. 4(a) lower two plots], can be easily explained by depolarization effects. The depolarization was in fact observed for the In-island layers on GaAs (Ref. 16) and was also calculated, for instance, for scatterers consisting of polystyrene spheres of different diameters.²² In case of a metal, one would expect this effect to be seen at smaller size parameters because of the higher absorption and refractive index caused by the polarizability of metals.

V. THREE-PHASE MODELING

In order to substantiate the above interpretation, we performed a modeling of the reflectance anisotropy spectra based on an effective-medium approach. A more quantitative modeling of the In-island system on GaAs would be an extremely complicated task, much beyond the scope of our work. Analytical expressions for the change of reflectivity induced by a rough surface are available only for certain simple geometries, which do not fit into the present situation.¹⁹ Semiquantitative numerical treatments of ensembles of particles with complex shapes are discussed in the literature, but limited to a relatively small number of scatterers.^{20,23,24} The low-symmetry shape, irregular size and orientation of the islands, and in particular, the extremely large number of islands precludes such a modeling for In on GaAs. A much simpler approach, however, is possible, based on an effective-medium model describing the island layer. Such a modeling is known to work well for small islands²¹ but will have only a limited accuracy in the Mie regime, relevant here.

The modeling is restricted to the dipole approximation as multipole resonances are not considered. A three-phase model consisting of a GaAs substrate, an In-island layer, and vacuum is employed to calculate the RAS spectra. The morphological anisotropy of the In-island layer is modeled on the basis of an effective medium consisting of In ellipsoids in a vacuum matrix. The calculation of the optical properties of metallic island films is performed in two steps: (1) Determination of an effective medium with oriented and coated el-

lipsoids. (2) Calculation of the optical response of a thin film using the effective medium and taking the multireflections into account by the Airy equation.

The measured RAS signal is identical to $\cos(2\Psi)$ (or Stokes parameter S_1) of the ellipsometric parameter Ψ , which is determined in step (2). The ellipsoids are oriented with the rotation axis parallel to the $[110]$ axis within the surface of the GaAs(001) substrate. The aspect ratio (ratio of major to minor axes), the complex refractive index of the core, the coating and the substrate, the thickness of the coating, and the refractive index of the surrounding medium are parameters of this calculation. Under these conditions, the effective optical constants for a given filling factor (ratio of mass and optical thickness) are determined by the Bruggeman approach,²⁷ using the resulting polarizability^{28,29} from the electrical depolarizations of the ellipsoids reported by Stoner.³⁰ The former theoretical approach was originally used to determine the optical properties of metallic island films coated with adsorbates.³¹ If the refractive index of the coating is the same as that of the surrounding medium, then the coating controls the minimum distance (twice the coating thickness) between the surfaces of the core ellipsoids. This is the case in our modeling approach. Thus, with the determined effective complex refractive index and the optical thickness of the coating layer on the GaAs substrate, the complex reflection is computed for the orientations parallel to the $[\bar{1}\bar{1}0]$ and $[110]$ directions. Since the model film is anisotropic, a different response for the two directions, corresponding to an RAS signal, follows. This holds both for a low angle of incidence and perpendicular incidence. The optical properties of GaAs and In bulk materials were taken from Refs. 25 and 26.

Figure 6 shows, as representative examples, calculated RAS spectra together with the corresponding experimental data for two different In coverages (150 ML, 350 ML). The fitting procedure is restricted to the coverage regime from 100 ML up to 600 ML, in which the first-order (dipole) oscillation 1-2 is visible in the RAS spectral range. Please note that oscillation 3-4 cannot be reproduced within our model since it is limited to the dipole resonance. Even though the use of ellipsoids for obelisk-like structures is a rather crude approximation to the real structure, since neither the complicated obelisk-like shape nor the finite-size distribution of the In islands is taken into account, a rather good agreement in the line shape between modeled and measured data is obtained for the oscillation 1-2. This finding corroborates well with a recent investigation of ensembles of complex particles by the extended boundary-condition method.²⁴ As mentioned above, in our modeling, the fitting parameters are the aspect ratio, the layer thickness, the island diameter, and the island distance. The aspect ratio which is a measure of the average geometric anisotropy of the island film turns out to be a very small, almost a constant value from 1.01 to 1.05 throughout all fitted RAS spectra of different In coverages. This finding corroborates very well with the island morphology, as revealed by SEM discussed in Sec. III A: Although the individual islands are anisotropic, they differ in shape and orientation, such that the average anisotropy is too small to be obvious just from visual inspection of the SEM images. Only

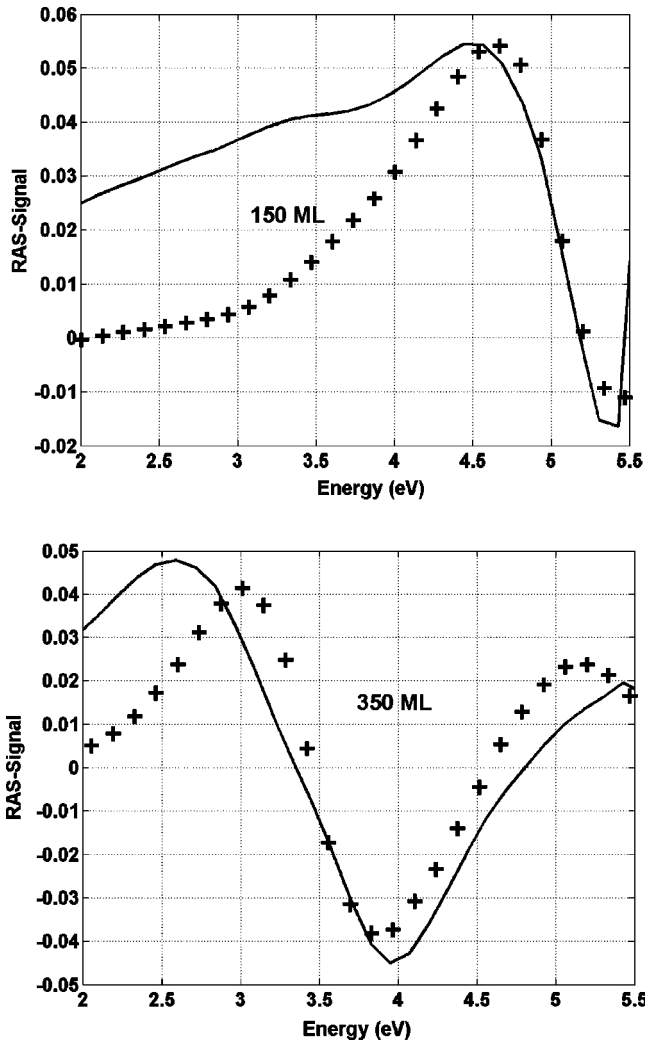


FIG. 6. Comparison of modeled (solid line) and experimental (cross symbols) RAS spectra for 150 ML (upper panel) and 350 ML (lower panel) of nominal In coverage. The modeling is based on a three-layer system with Bruggeman effective-medium approach for the indium-island layer. Multipole resonances are not taken into account.

the optical anisotropy proves that a small but well-defined average anisotropy, in fact, exists for the In-coverage regime examined. The fitting parameters layer thickness, island diameter, and the island distance show a pronounced dependence on In coverage which allows one to extract further information about island morphology. Figure 7 displays these parameters as obtained from our model fitting for indium coverage between 100 ML and 600 ML. The island film thickness shows a sublinear increase with In deposition. At 100 ML deposition (corresponding to 16.3 nm thickness of an ideally 2D In layer), the fitting yields a thickness of 100 nm, i.e., six times larger than for a 2D In layer. At 400 ML In deposition (65 nm nominal coverage), the film thickness is ≈ 200 nm, i.e., only three times larger than for a 2D film. These factors reflect the changes in growth mode of the In film as described in Sec. III A: Obelisklike shaped, isolated In islands aggregate and subsequently grow together. The initial factor of 6 accounts quantitatively for the low volume

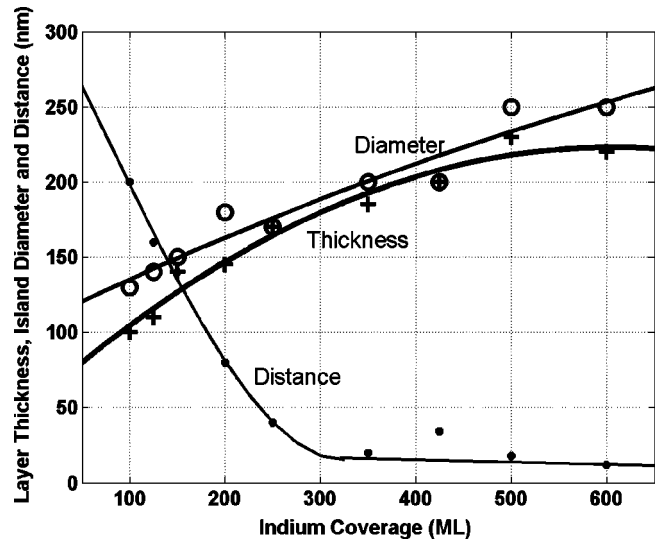


FIG. 7. Morphology parameters of the In-island film obtained on the basis of our three-phase modeling. Diameter of the In ellipsoids (open circles), distance of the ellipsoids (filled circles), and the thickness of the effective-medium film (cross symbols) are shown. The lines are a guide to the eye.

filling of the film achieved with the In islands. For higher coverage, the volume filling then increases. The island diameter resulting from our modeling shows an approximately linear increase with coverage up to 600 ML of In. Its nearly linear dependence on In coverage substantiates the interpretation of the RAS extremes in terms of geometric resonances since they, in fact, also show an approximately linear dependence on In coverage (see Fig. 5). The absolute value of the diameter is considerably smaller than, i.e., approximately half, the average island size revealed by SEM. However, the island sizes determined by SEM represent the island base. Since the island shape is obelisklike, the optically determined size should refer to a mean size obtained by averaging over the island cross sections within the whole In layer rather than at the island base. The distance between the islands, i.e., their spatial separation, decreases with increasing coverage up to 300 ML In coverage. For higher coverage, the distance is still not zero but at a small, almost constant value. This finding corroborates well with the evolution seen in the SEM images (see Sec. III A): Comparing 270 ML and 1000 ML of In coverage the island size is considerably increased for the latter, approximately by a factor of 3. The island distance, however, is not significantly reduced. At 1000 ML, we still see individual In islands, regardless of the fact that the island growth must have led to coalescence in between. As a consequence, by coalescence of adjacent islands, larger but still isolated islands have formed.

Summarizing, our effective-medium modeling based on In ellipsoids of a uniform size cannot account for the complex shape of the In islands and their size distribution. Qualitatively, however, the dependence of derived island diameter, island separation, and layer thickness upon In coverage reveals a good measure of the evolution of the true layer morphology.

VI. CONCLUSIONS

We have shown that strong resonances in reflectance anisotropy spectra for indium islands on GaAs(001) occur due to the island morphology. Surface-plasmon resonances related to the metal island structure lead to a strong enhancement of a small optical anisotropy which results from island sizes, shapes, and distribution by averaging over the illuminated area. The resonance wavelengths are directly linked with structural parameters of the metal islands. Thus, reflectance anisotropy spectroscopy provides a simple, reference-free optical tool to determine structure parameters (such as the size) of small particles. Statistical information

about the In-layer morphology, i.e., related to the mean island size, mean island distance, and layer thickness, can be obtained from an effective-medium modeling of the optical anisotropy.

ACKNOWLEDGMENTS

We gratefully acknowledge financial support by the Deutsche Forschungsgemeinschaft within Project No. B6 of the Sfb290. We also would like to thank U. Resch-Esser and the ZELMI at TU Berlin for the structural characterization of In islands.

*Corresponding author. FAX: ++49-(0)30-314-21769, Email address: norbes@gift.physik.tu-berlin.de

¹G. Mie, *Ann. Phys. (Leipzig)* **25**, 377 (1908).

²H. C. Hulst, *Light Scattering by Small Particles* (Wiley, New York, 1957).

³M. Kerker, *The Scattering of Light and Other Electromagnetic Radiation* (Academic Press, New York, 1969).

⁴R. Wannemacher, A. Pack, and M. Quinten, *Appl. Phys. B: Lasers Opt.* **68**, 225 (1999).

⁵I. Kamiya, D.E. Aspnes, L.T. Florez, and J.P. Harbison, *Phys. Rev. B* **46**, 15 894 (1992).

⁶W. Richter, *Philos. Trans. R. Soc. London, Ser. A* **344**, 453 (1993).

⁷A.I. Shkrebtii, N. Esser, W. Richter, W.G. Schmidt, F. Bechstedt, B.O. Fimland, A. Kley, and R. Del Sole, *Phys. Rev. Lett.* **81**, 721 (1998).

⁸Y. Borensztein, W.L. Mochan, J. Tarriba, R.G. Barrera, and A. Tadjeddine, *Phys. Rev. Lett.* **71**, 2334 (1993).

⁹J. Bremer, J.-K. Hansen, and O. Hunderi, *Surf. Sci.* **436**, L735 (1999).

¹⁰B. Sheridan, D.S. Martin, J.R. Power, S.D. Barrett, C.I. Smith, C.A. Lucas, R.J. Nicols, and P. Weightman, *Phys. Rev. Lett.* **85**, 4618 (2000).

¹¹T. Herrmann, K. Lüdge, W. Richter, N. Esser, P. Pouloupoulos, J. Lindner, and K. Baberschke, *Phys. Rev. B* **64**, 184424 (2001).

¹²U. Resch-Esser, N. Esser, C. Springer, J. Zegenhagen, W. Richter, M. Cardona, and B.O. Fimland, *J. Vac. Sci. Technol. B* **13**, 1672 (1995).

¹³U. Resch-Esser, N. Esser, D.T. Wang, M. Kuball, J. Zegenhagen, B.O. Fimland, and W. Richter, *Surf. Sci.* **352–354**, 71 (1996).

¹⁴C. Goletti, C. Springer, U. Resch-Esser, N. Esser, W. Richter, and B.O. Fimland, *Phys. Rev. B* **61**, 1681 (2000).

¹⁵S. Schintke, U. Resch-Esser, N. Esser, A. Krost, W. Richter, and B.O. Fimland, *Surf. Sci.* **377–379**, 953 (1997).

¹⁶U. Resch-Esser, N. Blick, N. Esser, Th. Werninghaus, U. Rossow, W. Richter, and Y. S. Raptis, in *Proceedings of the Fourth International Conference on Semiconductor Interface, Jülich*, edited by B. Lengeler, H. Lüth, W. Mönch, and J. Pollman (World Scientific, Singapore, p. 321).

¹⁷D. Aspnes, J.P. Harbison, A.A. Studna, and L.T. Florez, *J. Vac. Sci. Technol. A* **6**, 1327 (1985).

¹⁸P. Kratzer and M. Scheffler, *Phys. Rev. Lett.* **88**, 036102 (2002).

¹⁹D.E. Aspnes, *Phys. Rev. B* **41**, 10 334 (1990).

²⁰M. Quinten and U. Kreibitz, *Appl. Opt.* **32**, 6173 (1993).

²¹J.C. Pivin, M.A. Garcia, H. Hofmeister, A. Martucci, M. Sendova Vassileva, M. Nikolaeva, O. Kaitasov, and J. Llopis, *Eur. Phys. J. D* **20**, 251 (2002).

²²D. Bicout, C. Brousseau, A.S. Martinez, and J.M. Schmitt, *Phys. Rev. E* **49**, 1767 (1994).

²³V.N. Pustovit, J. A. Sotelo, and G.A. Niklasson, *J. Opt. Soc. Am. A* **19**, 513 (2002).

²⁴F.M. Kahnert, J.J. Stamnes, and K. Stamnes, *J. Opt. Soc. Am. A* **19**, 521 (2002).

²⁵P. Lautenschlager, M. Garriga, S. Logothetidis, and M. Cardona, *Phys. Rev. B* **35**, 9174 (1987).

²⁶U. Rossow, Ph.D. thesis, TU Berlin, 1993.

²⁷D.A.G. Bruggeman, *Ann. Phys. (Leipzig)* **24**, 636 (1935).

²⁸Y. Nishikawa, F. Fujiwara, K. Ataka, and M. Osawa, *Anal. Chem.* **65**, 556 (1993).

²⁹M. Osawa, K. Ataka, K. Yoshii, and Y. Nishikawa, *Appl. Spectrosc.* **47**, 1497 (1993).

³⁰E.C. Stoner, *Philos. Mag.* **7**, 803 (1945).

³¹A. Röseler and E.H. Korte, *Thin Solid Films* **313–314**, 732 (1998).